

---

# Raphael Painting Authentication and Style Transfer

---

Anonymous Author(s)  
Affiliation  
Address  
email

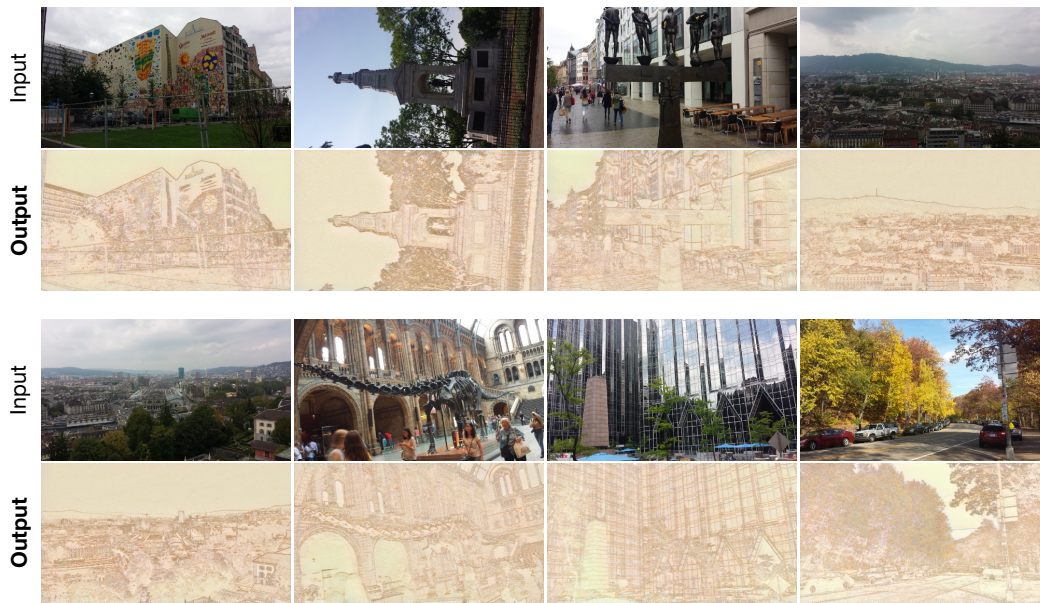


Figure 1: A quick view of our results in style transfer (you can zoom to see larger images)

## Abstract

1 Painting authentication and image style transfer are two essential but difficult image  
2 processing tasks. The major difficulty is to extract efficient features that represent  
3 a painting’s style. Here, we introduce two feature extracting methods to the first  
4 task: 1) a geometric tight frame with three statistics; 2) a style representation  
5 derived from a pre-trained CNN. Furthermore, we apply a forward feature selection  
6 algorithm and get satisfying results in authentication of Raphael’s paintings.

7 In the style transfer task, we implement Gatys’ Neural Algorithm of Artistic Style  
8 and improve it by preprocessing content image, such as contour extraction, edge  
9 enhancement and extracting the painter’s style from 12 genuine pictures. We also  
10 apply the Encoder-Decoder techniques like Discovery GAN. Our preprocessing  
11 techniques greatly improve the quality of output images, as they match more to  
12 Raphael’s sketch style and our attempt of applying Discovery GAN in this task is  
13 also successful.

# 1 Raphael Painting Authentication

## 1.1 Introduction

Art authentication is always a hard problem even for those experts of certain artist and worse yet, it sometimes costs a great amount of money, which may surpass the value of the painting itself, to apply high-techs, such as Isotope tracing and other chemical analysis.

Fortunately, with the rapid development of AI, especially in machine learning and deep learning, it is possible to do such authentication through relating algorithms without human interaction.

**Related work** Generally, there are two main methodologies in this field. One is stroke based [Elgammal et al., 2017], the other focuses on more general features [Liu et al., 2016, Li et al., 2017]. Considering the particular painting style of Raphael within our data, we will mainly follow the latter one in this paper.

## 1.2 Data

The data set is provided by Prof. Yang Wang, HKUST, which consists of high resolution scans of 28 paintings. The picture sizes are different from each other, ranging from 1192\*748 to 6326\*4457 pixels. Among the 28 paintings, 12 have been classified as genuine, 9 have been known to be forgeries, and remaining 6 are currently questioned by experts.

### 1.2.1 Data preprocessing

Note that some images of the raw data are stored as tiff files (images 2/3/4/5/6/8/9/24/27/28) while others are jpg files (images 11/12/13/14/15/16/17/18/19/21/22), the problem is that tiff files contains four channels which are RGBA (i.e. Red/Green/Blue/Alpha) and jpg files only contains the first three channels. However, after normalization, we also noticed that, in each image, every entry of the alpha channel equals to one. Hence, we assume it is safe to draw a conclusion that alpha channel doesn't affect much in this task.

After a quick skim through the dataset, we make a note about the boundary of the paintings here. Since almost every painting is centered, intuitively we would agree that the edges of the canvas in the paintings may not be useful information for art authentication, and hence we have excluded these edges in our numerical experiments. More precisely, for each painting in the dataset, we crop off 100 pixels from its four sides, and use only the interior of the image in our numerical tests.

Talking about doing data augmentation, in order to make up for the small size of dataset, we use two methods to cut images, one is to cut raw image into small patches by specified pixel size (e.g.  $227 \times 227$ ), another is to cut it by specified number of patches (e.g. 16 patches per image). Also, for the purpose of avoiding situations like we crop a component object into two parts, we allowed 20% overlapping area when cropping. The procedure mentioned above is shown in Figure 2.

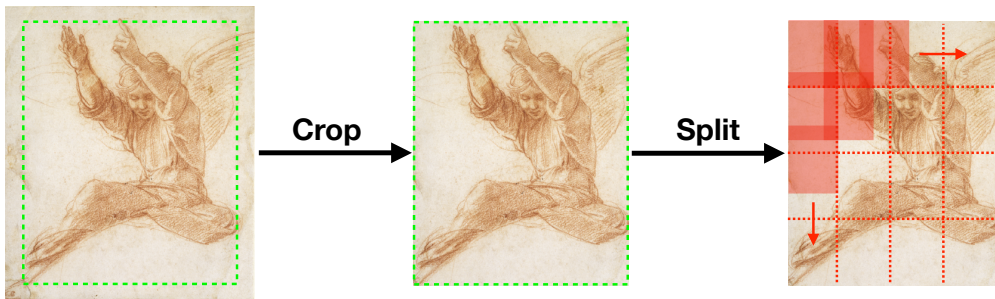


Figure 2: Data preprocessing example

46

47 To apply the geometric tight frame of Li et al. [2010] and Li et al. [2011], we first turn the pictures  
48 into grey-scale images with one channel.

49 Normally, the tight frame is applied on grey-scale images with format ‘uint8’, of which any pixel  
50 ranges from 0 to 255. Here, we are curious about those constant coefficients of the tight frame and  
51 thus, we try on another format of the images, ‘float’, of which any pixel ranges from 0-1. The latter  
52 one performs better after forward stage-wise feature selection.

### 53 1.3 Basic Method

#### 54 1.3.1 Feature extraction

55 The feature extraction procedure here is the same as that of Liu et al. [2016].

56 What’s more, we find that because of the specificity of our training data, the image matrix is ‘sparse’  
57 to some extent. And this problem is even worse if we apply the geometric tight frame. That is to say  
58 a certain amount of features are close to zero, which is a nightmare to some classifiers. So, we apply  
59 standardization to the features (rescale to mean 0 and standard error 1).

60 In summary, together with the data preprocessing procedures, we will have mainly two groups  
61 of features: patch or no-patch, each of which has four type of features: ‘uint8’ or ‘float’ and  
62 standardization or not. Note that re-encode an image from uint8 to float is the same as normalization.  
63 So the name of these different features are just like what’s shown in Figure 3 & 4.

#### 64 1.3.2 Training procedure

65 The main idea of this classification task is outlier detection [Liu et al., 2016]. With the intuition  
66 that the genuine ones will ‘gather together’ while the fake ones would be more ‘far away’. So the  
67 classifier is built mainly on the Euclidian distance, which is also called ‘2-norm’.

68 The main procedure here could be summarized as three steps: (more details please refer to Liu et al.  
69 [2016])

- 70 • get the ‘genuine center’ of training data
- 71 • get the threshold of the distance from one sample to the center
- 72 • label the validation data with the center and the threshold

73 Note that our training data is limited (only 21 pictures without augmentation). So here we simply  
74 apply the leave-one-out cross validation(LOOCV) procedure to avoid overfitting problem.

#### 75 1.3.3 Feature selection

76 In previous part, we induce totally 54 features for each grey-scale image. Intuitively, there would  
77 be some noise within so many features. That is to say, fewer features can perform better for this  
78 classification task.

79 Speaking of feature selection algorithms, there are also two main methodologies, forward selection  
80 and backward selection. For computational efficiency, we choose the forward one. While for the rank  
81 boosting algorithm proposed by Liu et al. [2016], we think it may not suit the problem well enough.  
82 A good reason is that *artistic authentication* is not a recognition problem, of which the dominant  
83 features can do most of the job. But for authentication, sometimes a group of sub-dominant features  
84 do help.

85 So, we propose a more direct forward selection algorithm based on the LOOCV. (see Table 1)

86 The results of feature selection on different type of features can be seen in Figure 3, in which we can  
87 clearly conclude that there are much noise in all 54 features because as the number of features grows,  
88 the performance generally goes down.

### 89 1.4 Other Potential Methods

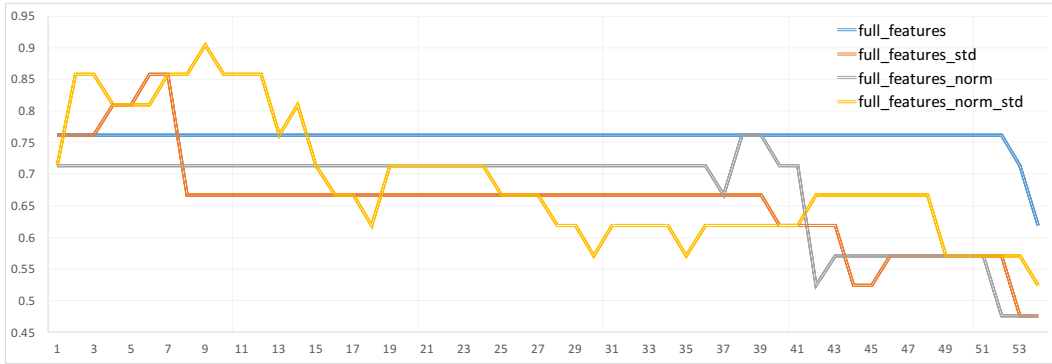
#### 90 1.4.1 Classic classifiers

91 Here we try other classic classifiers, such as KNN, SVM and decision tree, during which we introduce  
92 data augmentation by cutting the original images into 16 patches. (see section 1.2.1) We have a good

Table 1: forward selection algorithm

<b>Input</b>	$current\_set \leftarrow \emptyset$ $X \leftarrow (21,54)$ data matrix
<b>loop</b>	$i$ from 1 to 54: $remain\_set \leftarrow \{0, 1, 2, \dots, 53\} - current\_set$ <b>loop</b> $j$ in $remain\_set$ : $F_j \leftarrow current\_set \cup \{j\}$ $p_j \leftarrow$ the performance by LOOCV using $F_j$ <b>end</b> $j^* \leftarrow argmax_j \{p_j\}$ $P_i \leftarrow p_{j^*}$ $current\_set \leftarrow current\_set \cup \{j^*\}$
<b>end</b>	$best\ number\ of\ features \leftarrow argmax_i \{P_i\}$ and it's easy to get the corresponding features.

Figure 3: Performance of different number of features



93 reason that these classifiers' performance will grow with the increase in the volume of data. The  
 94 results of this part are in Figure 4.

#### 95 1.4.2 Style Feature Method

96 **Introduction** It is widely acknowledged that Convolutional Neural Networks(CNN) can capture  
 97 local information of a picture like brushwork, textures which we generally call style. Gatys et al.  
 98 [2016] introduced a neural algorithm of artistic style that can render a the semantic content of an  
 99 image into a different style with CNN. The main idea is that a pre-trained CNN (e.g VGG-19) can  
 100 extract high-dimension features in a given picture. The model introduced by Gatys et al. [2016] uses  
 101 features generated by CNN filters as content representation, the Gram matrixes as style representation  
 102 and also uses Gradient Descent to learn a picture with small content loss and style loss between  
 103 output and the target content and style.

104 **Model** In the task of authentication of paintings, it is natural to implement this idea in the process  
 105 of feature extraction because we want to determine based on information of the painter's style rather  
 106 than the painting's content. We believe that Gram matrixes, which consist of the correlation between  
 107 the different filter responses, can remove the content information, because every point in a Gram  
 108 matrix represent not a local but a global feature of the picture. Thus, they can dig deep into the  
 109 picture's information. More Details will be shown in the latter part of style transfer.

110 Like Gatys et al. [2016], we use VGG-19 as our pre-trained network, and use Gram matrixes 'conv1',  
 111 'conv2', 'conv3', 'conv4' and 'conv5' as style features. We reshape the Gram matrixes into a vector  
 112 and concatenate them into a long vector, which we use as style features. The network architecture is  
 113 shown in Figure 5.

Figure 4: Best performance of different classic model

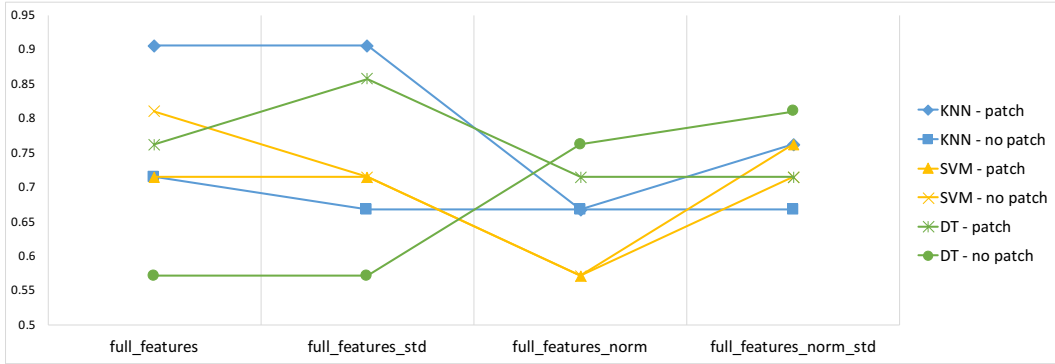
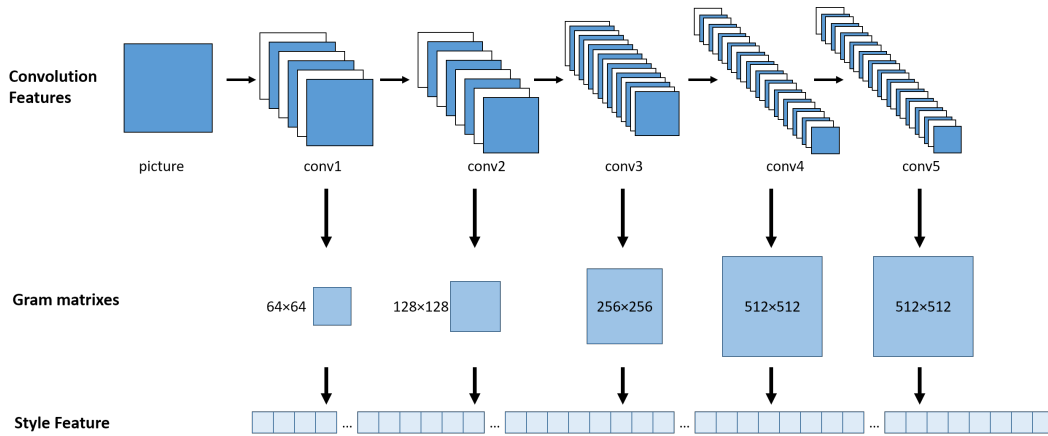


Figure 5: Process to extract style features



114 **Experiments** Then we apply K-Nearest Neighbours (KNN), Support Vector Machine (SVM) and  
 115 Decision Tree classifiers with leave-one-out validation. Due to memory constraint, we resize the  
 116 picture to 256/512/1024 pixels. We divide the picture into 16 patches in KNN classifier to augment  
 117 training data. The result is shown in Table 2. We find that since the dimension is too high (above  
 118 100,000), SVM is not applicable. KNN performs better on features got from low-definition pictures  
 119 with 16 separated patches and Decision Tree performs better on features got from low-definition  
 120 pictures.

Table 2: Leave-one-out result with style features

Feature Extraction	Model	TPR	TNR	Classification Accuracy
Style Features-256	KNN	0.833	0.889	<b>0.857</b>
	SVM	1.000	0.000	0.571
	Decision Tree	0.667	0.556	0.619
Style Features-512	KNN	1	0.333	0.714
	SVM	1.000	0.000	0.571
	Decision Tree	0.833	0.889	<b>0.857</b>
Style Features-1024	KNN	0.667	0.444	0.571
	SVM	1.000	0.000	0.571
	Decision Tree	0.833	0.889	<b>0.857</b>

121 **Predictions** Upon our style-features models, we give our prediction to the 7 pictures remain  
 122 disputed (Pic1/7/10/20/23/25/26). We pick three Models performed best in validation. We predict

123 that Picture 10/25 are genuine, and Picture 1/7/20 are counterfeit. For picture 23/26, our results varies,  
 124 so we have reservations about it. The result is shown in Table 3 (0 means counterfeit and 1 means  
 125 genuine).

Table 3: Predictions upon style-features models

	Pic1	Pic7	Pic10	Pic20	Pic23	Pic25	Pic26
Style Features-256 with KNN	0	0	1	0	0	1	0
Style Features-512 with Decision Tree	0	0	1	0	1	1	1
Style Features-1024 with Decision Tree	0	0	1	0	1	1	0

## 126 1.5 Baseline and Main results

127 **Baseline** Our baseline mainly comes from the work of Li et al. [2017], for their dataset is the same.

Table 4: Our final results of different models with different feature extractions

Feature Extraction	Model	TP	TN	Classification Accuracy
Tight Frame	Forward Stage-wise	83.3%	100%	<b>90.5%</b>
	SVM	83.3%	77.8%	81.0%
	Decision Tree	83.3%	88.9%	85.7%
	KNN	91.7%	88.9%	<b>90.5%</b>
Style Features	Decision Tree	83.3%	88.9%	85.7%
	KNN	83.3%	88.9%	85.7%

128 **Our final results (see Table 4)**

Table 5: Predictions of the two best models in Table 4

	Pic1	Pic7	Pic10	Pic20	Pic23	Pic25	Pic26
Forward Stage-wise	1	0	1	1	1	1	1
KNN	1	0	1	0	1	0	1

129 **Our conclusion on the 7 disputed paintings** Our final prediction on the 7 disputed paintings are  
 130 based on a voting model, which is a combined model of the two most successful model in Table 4  
 131 and the style feature model in section 1.4.2. The rule is that only if the two model both give positive  
 132 prediction then the test image will be predicted as genuine painting. Otherwise, we will refer to the  
 133 predictions of style feature model in Table 3.

134 Based on this, we conclude that picture 1/10/23/25/26 are probably genuine and picture 7 is probably  
 135 a forgery.

## 136 1.6 Remaining problems and Future work

### 137 Remaining problems

- 138 • The reason why the features extracted by the tight frame and those three statistics work still  
 139 remains unknown.
- 140 • Also, the predictions given by different models vary from each other, of which the predicting  
 141 criterion varies from each other.

### 142 Future work

- 143 • Apart from the tight frame, other frames should be explored and tested to help find out the  
 144 reason for the ability of authentication.

- The style features extracted in section 1.4.2 also do a good job. However, the number of total features is over 100,000. So an efficient feature selection algorithm should be designed to reduce those noise features.

## 2 Raphael Artistic Style Transfer

### 2.1 Introduction

Before the advent of Neural Network, to transfer a style is to establish a mathematical model to extract the style information and then apply this model to a content image. Despite that such work can do a style transfer task, it is restrained by the certain style and certain mathematical model. If the style image changes, people need to go over the whole work again.

This phenomenon changes greatly after the work of Gatys et al. [2016], which will be the main reference to our work in this paper.

**Related work** In recent years, Deep Convolutional Neural Networks (CNN) [Krizhevsky et al., 2012] has attracted many attention because of its deep features generated ability. Zeiler and Fergus [2013] has been shown in high-level image recognition tasks that such deep features are better representations for images. This inspired work on neutral style transfer [Gatys et al., 2016], which successfully applied CNN (pre-trained VGG-16 networks [Zeiler and Fergus, 2013] to the problem of style transfer, or texture transfer [Gatys et al., 2015].

Style transfer is used as a means to migrate an artistic style from an example image to a source image. The decomposition of content and style in artistic images is bound to the coupling between the source content and the example style. Using CNN architecture is able to produce more impressive stylization results than traditional texture transfer, since a CNN is effective in decomposing content and style from images. Selim et al. [2016] further extended this idea to portrait painting style transfer by adding face constraints. The most related work to ours is patch-based style transfer by combining a Markov Random Field (MRF) and a CNN [Li and Wand, 2016].

Generative adversarial networks (GAN) [Goodfellow et al., 2014] are a powerful class of generative models that cast generative modeling as a game between two networks: a generator network produces synthetic data given some noise source and a discriminator network discriminates between the generator's output and true data. GANs can produce very visually appealing samples, and it has many applications: estimating a high-resolution (HR) image from its low-resolution (LR) counterpart which can be referred to as super-resolution (SR) [Ledig et al., 2016], scene understanding including scene object retrieval [Gulrajani et al., 2017] and image-to-image translation [Isola et al., 2017].

### 2.2 Basic Method

Our basic algorithm for style transfer comes from the main idea of Gatys et al. [2016], in which a pre-trained deep convolutional neural network (in our paper is VGG19) is introduced to extract the information of style from the style image as well as the content from content image.

- **content loss**

Let  $X$  be our input data matrix, and then  $F_{XL}$  is denoted as the features at layer  $L$ . So input data  $X$ 's content information at layer  $L$  is determined by  $F_{XL}$ . And if we have our target content image  $X$  and the image  $Y$  that we want to reconstruct, the content loss of  $Y$  at layer  $L$  w.r.t  $X$  is defined as follows.

$$\mathcal{L}_{content}^L(Y, X) := \left\| F_{YL} - F_{XL} \right\|_2^2 \quad (1)$$

- **style loss**

Again, for image  $X, Y$  at layer  $L$ , we have the features  $F_{XL}, F_{YL}$  respectively. First, the style information of  $X$  at layer  $L$  is defined as follows ( $Y$  is similar).

$$\begin{aligned} \mathcal{I}_{style}^L(X) &:= \left( G_{XL}(i, j) \right)_{K_L \times K_L} \\ G_{XL}(i, j) &:= \langle F_{XL}^i, F_{XL}^j \rangle \end{aligned} \quad (2)$$

188 where  $F_{XL}^i$  is denoted as the vectorized  $i^{th}$  feature of the X-features at layer  $L$ ,  $K_L$  is  
 189 denoted the number of vectorized features at layer  $L$ , which means  $G_{XL}$  is a  $K_L \times K_L$   
 190 matrix, and  $\langle, \rangle$  is denoted as the inner product of two vectors.  
 191 Then the style loss of image  $Y$  w.r.t image  $X$  at layer  $L$  is defined as follows.

$$\mathcal{L}_{style}^L(Y, X) := \left\| \mathcal{I}_{style}^L(Y) - \mathcal{I}_{style}^L(X) \right\|_2^2 = \left\| G_{YL} - G_{XL} \right\|_2^2 \quad (3)$$

192 The total loss is defined as the linear combination of the loss of content and style [Gatys et al., 2016].

$$\mathcal{L}_{total} = \alpha \mathcal{L}_{content} + \beta \mathcal{L}_{style}$$

193 So during the back-propagation, the gradient of  $Y$  at layer  $L$  is the linear combination of the content  
 194 and style.

$$\nabla_L(Y, X_C, X_S) = \alpha_L \nabla_L(Y, X_C) + \beta_L \nabla_L(Y, X_S) \quad (4)$$

$$\nabla_{total}(Y, X_C, X_S) = \sum_{L_C} \alpha_{L_C} \nabla_{L_C}(Y, X_C) + \sum_{L_S} \beta_{L_S} \nabla_{L_S}(Y, X_S) \quad (5)$$

195 where  $L_C, L_S$  are the layers that determines content and style, respectively, and  $\alpha_{L_C}, \beta_{L_S}$  are  
 196 corresponding weights.

197 Here, we simply take uniform weights.[Gatys et al., 2016] That is to say,

$$\forall L_C, \alpha_{L_C} = \alpha; \quad \forall L_S, \beta_{L_S} = \beta$$

198 More details about the layers that determines content and style will be covered in the following  
 199 section, as well as the choice of weights,  $\alpha$  &  $\beta$ .

200 Unlike the traditional training procedure of Neural Network, the back-propagation process here aims  
 201 to *reconstruct* the output image other than the parameters within the network layers.

202 Note that those successful results in Gatys et al. [2016], Liao et al. [2017], Chen and Koltun [2017]  
 203 and many others have been a testament to the capability of CNN network to extract the information  
 204 of style and content from a certain image. Still, the reason of CNN's such ability remains unknown,  
 205 for the information of style is something subjective. The ultimate tool to test whether an image's  
 206 style is the same as the other one mostly depends on people's eyes and visual perception.

### 207 2.2.1 Basic version (Multi-color)



Figure 6: the basic version of style transfer

208 From Figure 6 we could see that the reconstructed image still looks like a photograph instead of a  
 209 real art work of Raphael. To find the reason, we may take a closer look at the deep convolutional  
 210 neural network.

211 So from Figure 7 we could see that the reconstructed content image remains most of information of  
 212 the input content image, including the objects and the colors. Meanwhile, the reconstructed style  
 213 image also resembles the input style image a lot, which can be another testament to the study of  
 214 Gatys et al. [2016].

215 However, one problem is obvious: the color. Note that the artistic style of Raphael within our dataset  
 216 is the same as the second picture in Figure 6. (Other styles of Raphael please refer to the section of  
 217 further discussion) And so, the image that we synthesized should be single-color, like the style image,  
 218 instead of the multi-color version.



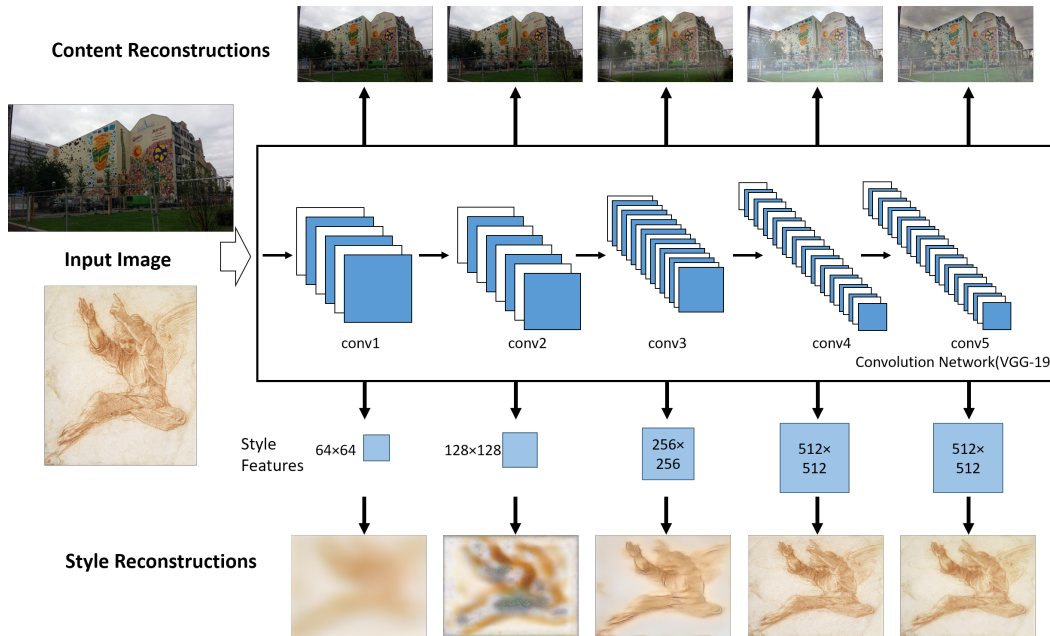


Figure 7: Detailed deep convolutional neural network

219 **Remarks:**

- 220
- 221
- 222
- 223
- 224
- 225
- 226
- Because the artistic style of Raphael within our dataset is not so strong as that of *Starry Night* by Vincent van Gogh, our weights are chosen to focus more on content:  $\alpha = 4$  &  $\beta = 1000$ , compared to  $\alpha = 1$  &  $\beta = 1000$  in Gatys et al. [2016].
  - Choice of different style image affects little on the synthesized image. It only changes the color as you can see in Figure 8. So we default the style image to be the same in our paper (and also we default the content image to be the same). If you want to see our results using other style images and other content images, please refer to section 2.5.2.

227 **2.2.2 Advanced version (Single-color)**

228 To deal with the problem of multi-color, we introduce some image preprocessing techniques. (see  
229 Figure 9)

230 From Figure 9 we can say that we've almost done the style transfer work. While if you are careful  
231 enough, you may find that there are still some little defects, such as the 'missing cloud' and the  
232 'hollow tree'. (see Figure 10)

233 **2.3 Another Potential Method: Discovery GAN**

234 DiscoGAN [Kim et al., 2017] is a method based on GAN that learns to discover relations between  
235 different domains. Using the discovered relations, it is capable of successfully transferring style from  
236 one domain to another while preserving key attributes such as orientation. Hugely inspired by this  
237 work, we tried this architecture on our Raphael artistic style transfer task, wondering if we can get  
238 some unexpected achievements.

239 **Results and Analysis** As we crop images into small pieces, the smaller these pieces are, the big  
240 dataset we will get. Hence, details of the four dataset are: 5854 images and  $227 \times 227$  for each image,  
241 673 images and  $600 \times 600$  for each image, 210 images and  $1000 \times 1000$  for each image, 10 raw  
242 images and each image's size varies.

243 Results can be concluded in Figure 11 (Note that in order to present the results, we resize them to  
244  $600 \times 600$ ). We can clearly see that performances of DiscoGAN are not as good as the performances  
245 of Gatys et al. [2016] since all these pictures are blur and insufficient of details. However, among these

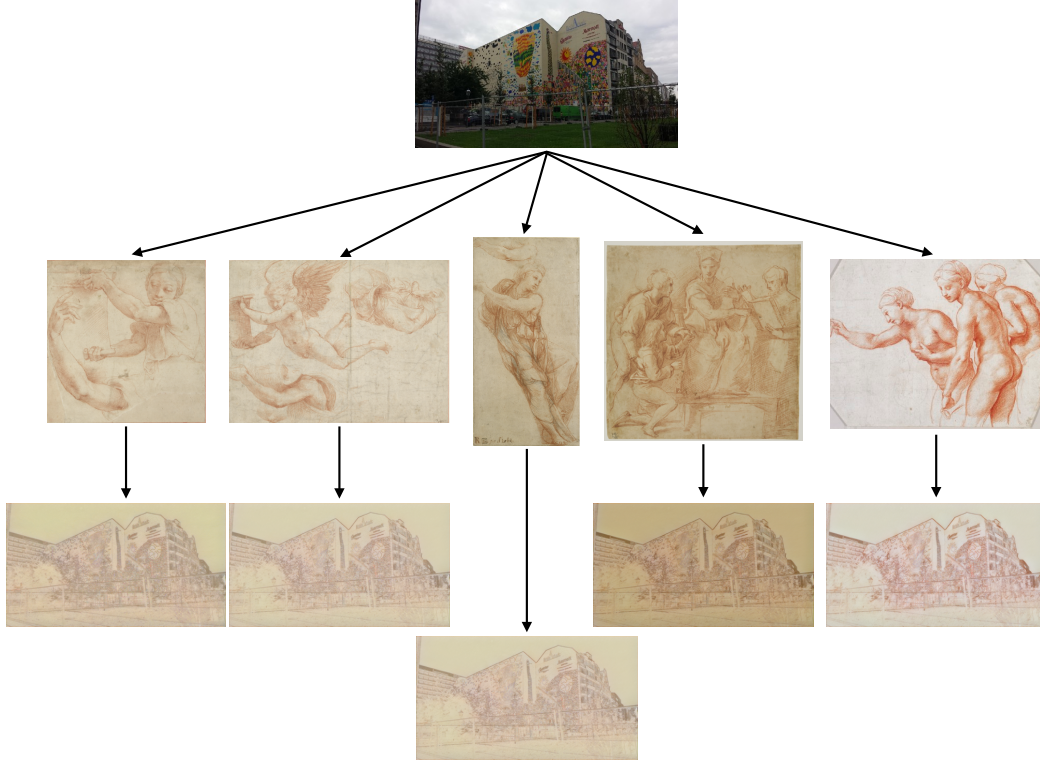


Figure 8: The effects of different input style image

246 four pictures, we are surprised to find out that both image size and dataset size play an important role  
 247 in this task. For example,  $600 \times 600$  dataset (with middle image size and middle dataset size) achieves  
 248 the best performance while  $227 \times 227$  dataset (with the smallest image size but the largest dataset)  
 249 and raw dataset (with the largest image size but the smallest dataset) both have poor performances.

250 Reasons of such performances may be explained as follows. It's easy to collect two styles of pictures,  
 251 while it's hard to capture two styles of pictures that represent exactly the same content. In our  
 252 unpaired pictures, a large amount of data is needed to fully learn features of training data. Otherwise  
 253 the model may not be good enough and may learn some noise data instead.

## 254 2.4 Our Results

255 A quick view of our final results can be seen in Figure 1. The full results images can be downloaded  
 256 from the URL<sup>1</sup>. (Note that there are more than 1000 images in all.)

## 257 2.5 Further Discussion

### 258 2.6 Average Painter's style

259 In the experiment above we always pick one content picture and one style picture and make a one-one  
 260 combination. However, in this case, we always transfer the content picture to a certain painting's style  
 261 but not the painter, Raphael's style. From this point of view, we want to find a way to accomplish the  
 262 task of style transfer using all 12 genuine Raphael's paintings.

263 From the model above, we represent a picture's style by the Gram matrixes of the feature space in  
 264 different convolutional layers. So we can take the average of style features of 12 genuine paintings,  
 265 use it as the painter's style and take it as the target style features to compute the style loss (MSE).  
 266 Since the target style is fixed in the training process, this approach is feasible.

<sup>1</sup><https://pan.baidu.com/s/1i6KBpNf> and the password is *jkwg*

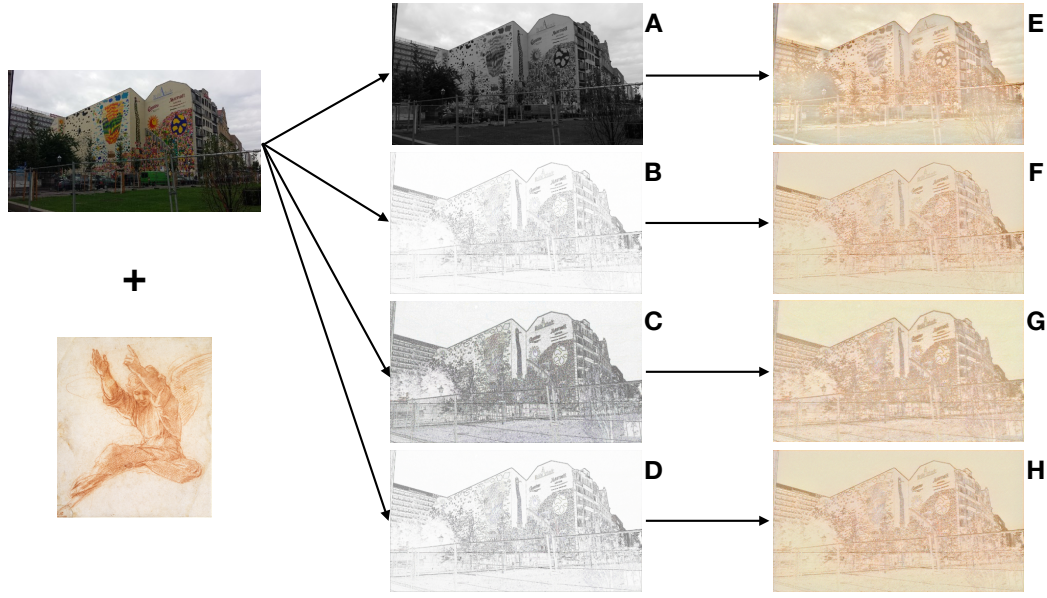


Figure 9: Here are four image preprocessing techniques: grey-scale, contour extraction, edge enhancement and sharpening. Image A, B, C, D are the content images after applying the four techniques, respectively, and image E, F, G, H are the corresponding synthesized images.

267 We implement this method on the test images and the result is shown in Figure 12. We compare the  
 268 output trained from average features and one-picture features and find that average features are a  
 269 more stable way to transfer to the painter’s style and are available to get a picture more like a painting  
 270 rather than still a photo.

### 271 2.6.1 Other artistic style transfer demo

272 We have applied our style transfer model using other famous artist’s paintings. (see Figure 13) It  
 273 turns out that our model performs well.

### 274 2.6.2 The problem of resolution

275 As mentioned in Gatys et al. [2016], a serious problem of style transfer is about image resolution. That  
 276 is to say, the synthesized image is always small in size. (In our experiment, the size of synthesized  
 277 image is  $512 \times 910$ )

278 Related work can be summarized as the algorithms, such as SCRNN[Hsu, 2009], ESPCN and  
 279 DRCN[Chen and Koltun, 2017]. And there are some resolution work on photographs using  
 280 GAN.[Ledig et al., 2016]

281 However, we find that the resolution algorithms mentioned in these articles are all about to deal with  
 282 very small pictures and the size of output image are no greater than  $512 \times 512$ . So compared to our  
 283 output image size  $512 \times 910$ , we think they won’t be helpful to our results.



Figure 10: Some little defects. Here we mainly have two defects. One is shown as image C2, E1, E2 and G1, which can be concluded as detail loss. The other is presented in image C1, which can be concluded as object loss. The previous one can be attributed to the mistiness of the input image (see A2, D1, D2 and F1). While the latter one is a shortage of the image preprocessing techniques. We can see that the result with grey-scale input B performs better with both the clouds(B1) and the tree(B2). However, the problem is again the color. Till ddl, we are still not sure why a grey-scale input content can lead to a color like green(B2). Nevertheless, we still choose images like C to be our final results. (see Figure 1)

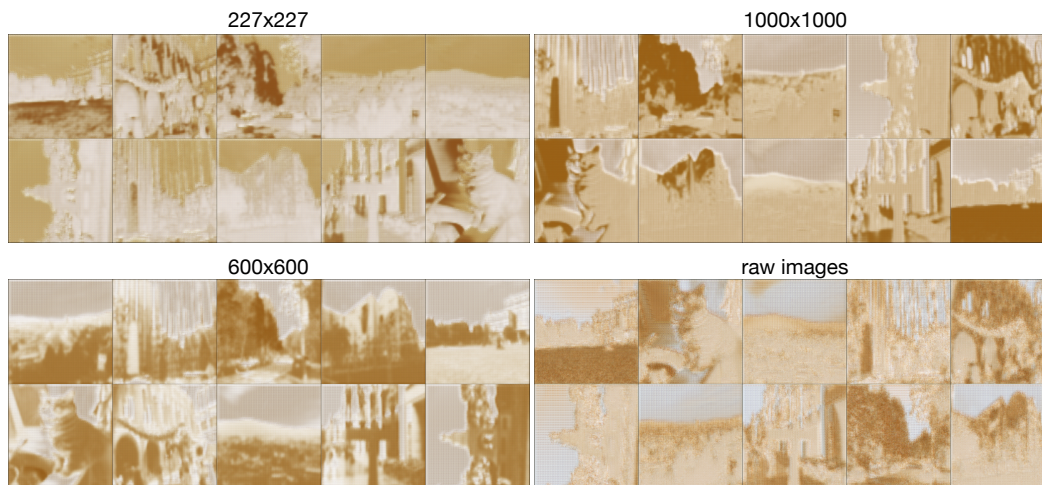


Figure 11: different performances under different sizes of training image (DiscoGAN)



Figure 12: Comparison of using one-picture features and average-features

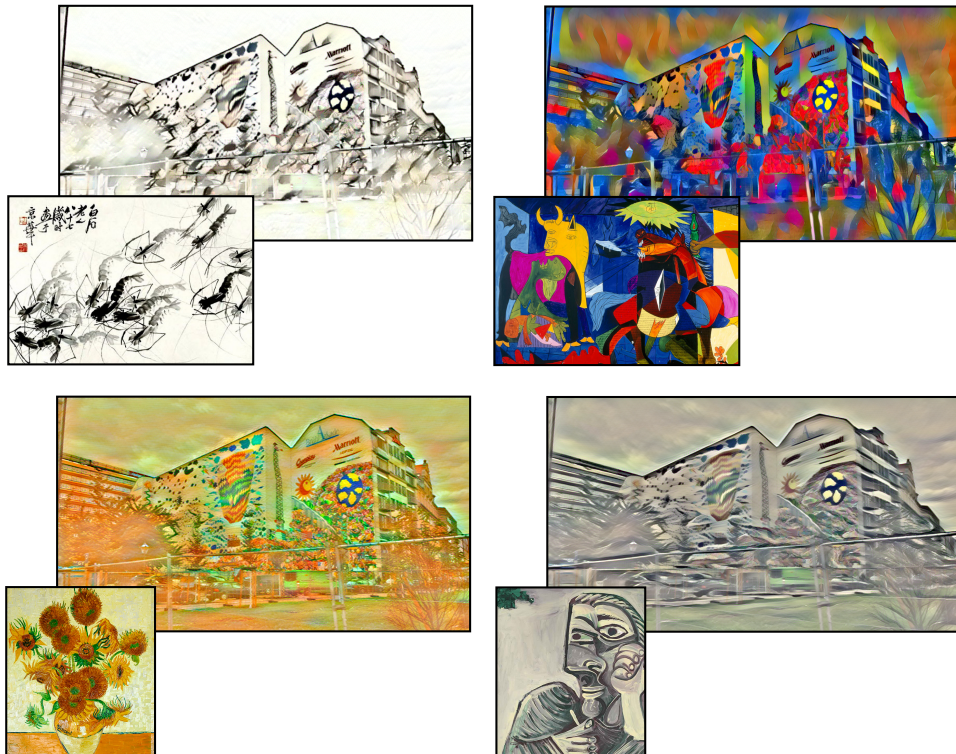


Figure 13: Other artistic style transfer demo. Top left is from Baishi Qi's *Shrimp*; top right is from Picasso's *Guernica*; down left is from Van Gogh's *Sunflowers*; down right is from Picasso's *Self portrait*.

284 **References**

- 285 Qifeng Chen and Vladlen Koltun. Photographic image synthesis with cascaded refinement networks.  
286 In *The IEEE International Conference on Computer Vision (ICCV)*, volume 1, 2017.
- 287 Ahmed Elgammal, Yan Kang, and Milko Den Leeuw. Picasso, matisse, or a fake? automated analysis  
288 of drawings at the stroke level for attribution and authentication. *arXiv preprint arXiv:1711.03536*,  
289 2017.
- 290 Leon A Gatys, Alexander S Ecker, and Matthias Bethge. Texture synthesis using convolutional neural  
291 networks. *Febs Letters*, 70(1):51–55, 2015.
- 292 Leon A Gatys, Alexander S Ecker, and Matthias Bethge. Image style transfer using convolutional  
293 neural networks. In *Computer Vision and Pattern Recognition (CVPR), 2016 IEEE Conference on*,  
294 pages 2414–2423. IEEE, 2016.
- 295 Ian J. Goodfellow, Jean Pouget-Abadie, Mehdi Mirza, Bing Xu, David Warde-Farley, Sherjil Ozair,  
296 Aaron Courville, and Yoshua Bengio. Generative adversarial nets. In *International Conference on*  
297 *Neural Information Processing Systems*, pages 2672–2680, 2014.
- 298 Ishaan Gulrajani, Faruk Ahmed, Martin Arjovsky, Vincent Dumoulin, and Aaron C Courville.  
299 Improved training of wasserstein gans. In *Advances in Neural Information Processing Systems*,  
300 pages 5769–5779, 2017.
- 301 Chun Fei Hsu. Intelligent position tracking control for lcm drive using stable online self-constructing  
302 recurrent neural network controller with bound architecture. *Control Engineering Practice*, 17(6):  
303 714–722, 2009.
- 304 Phillip Isola, Jun-Yan Zhu, Tinghui Zhou, and Alexei A Efros. Image-to-image translation with  
305 conditional adversarial networks. *arXiv preprint*, 2017.
- 306 Taeksoo Kim, Moonsu Cha, Hyunsoo Kim, Jungkwon Lee, and Jiwon Kim. Learning to discover  
307 cross-domain relations with generative adversarial networks. *arXiv preprint arXiv:1703.05192*,  
308 2017.
- 309 Alex Krizhevsky, Ilya Sutskever, and Geoffrey E. Hinton. Imagenet classification with deep convolu-  
310 tional neural networks. In *International Conference on Neural Information Processing Systems*,  
311 pages 1097–1105, 2012.
- 312 Christian Ledig, Lucas Theis, Ferenc Huszár, Jose Caballero, Andrew Cunningham, Alejandro  
313 Acosta, Andrew Aitken, Alykhan Tejani, Johannes Totz, Zehan Wang, et al. Photo-realistic single  
314 image super-resolution using a generative adversarial network. *arXiv preprint*, 2016.
- 315 Chuan Li and Michael Wand. Combining markov random fields and convolutional neural networks  
316 for image synthesis. In *IEEE Conference on Computer Vision and Pattern Recognition*, pages  
317 2479–2486, 2016.
- 318 Yan-Ran Li, Dao-Qing Dai, and Lixin Shen. Multiframe super-resolution reconstruction using sparse  
319 directional regularization. *IEEE Transactions on Circuits and Systems for Video Technology*, 20  
320 (7):945–956, 2010.
- 321 Yan-Ran Li, Lixin Shen, Dao-Qing Dai, and Bruce W Suter. Framelet algorithms for de-blurring  
322 images corrupted by impulse plus gaussian noise. *IEEE Transactions on Image Processing*, 20(7):  
323 1822–1837, 2011.
- 324 Yue Li, Jinglin Chen, Shijie Cui, and Yuxuan Zhou. Artistic authentication of raphael paintings.  
325 2017.
- 326 Jing Liao, Yuan Yao, Lu Yuan, Gang Hua, and Sing Bing Kang. Visual attribute transfer through  
327 deep image analogy. *arXiv preprint arXiv:1705.01088*, 2017.
- 328 Haixia Liu, Raymond H Chan, and Yuan Yao. Geometric tight frame based stylometry for art  
329 authentication of van gogh paintings. *Applied And Computational Harmonic Analysis*, 41(2):  
330 590–602, 2016.

- 331 Ahmed Selim, Mohamed Elgharib, and Linda Doyle. Painting style transfer for head portraits using  
332 convolutional neural networks. *Acm Transactions on Graphics*, 35(4):1–18, 2016.
- 333 Matthew D. Zeiler and Rob Fergus. Visualizing and understanding convolutional networks. 8689:  
334 818–833, 2013.